Electronic Supplementary Material (ESI) for Dalton Transactions.

Supporting Information

Table of Contents

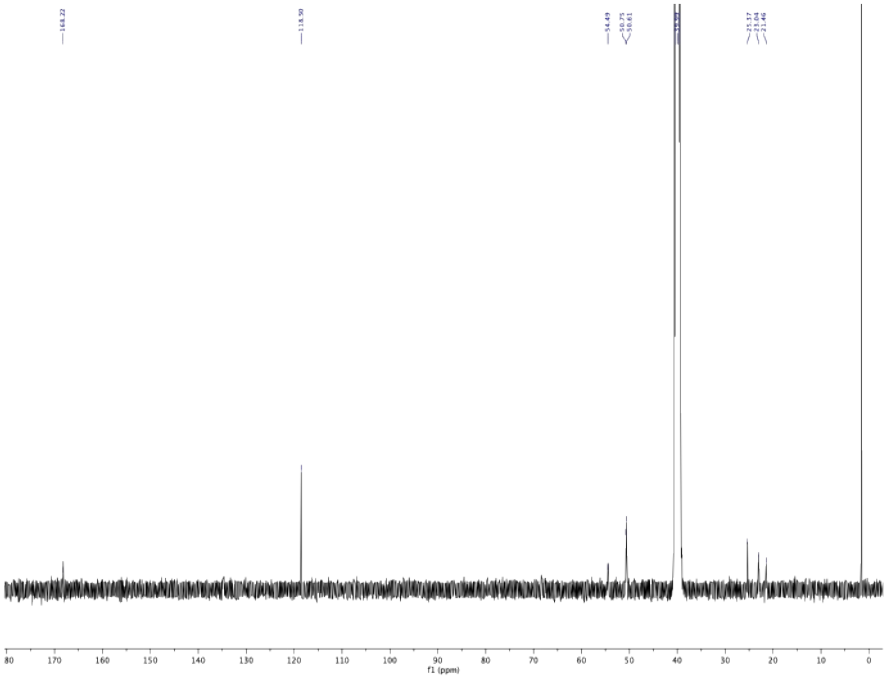

Figure S1. ^{13}C NMR spectrum of **Cu$^{(I)}$(H$_2$NSNS2A)** in DMSO-d$_6$ at 25°C.

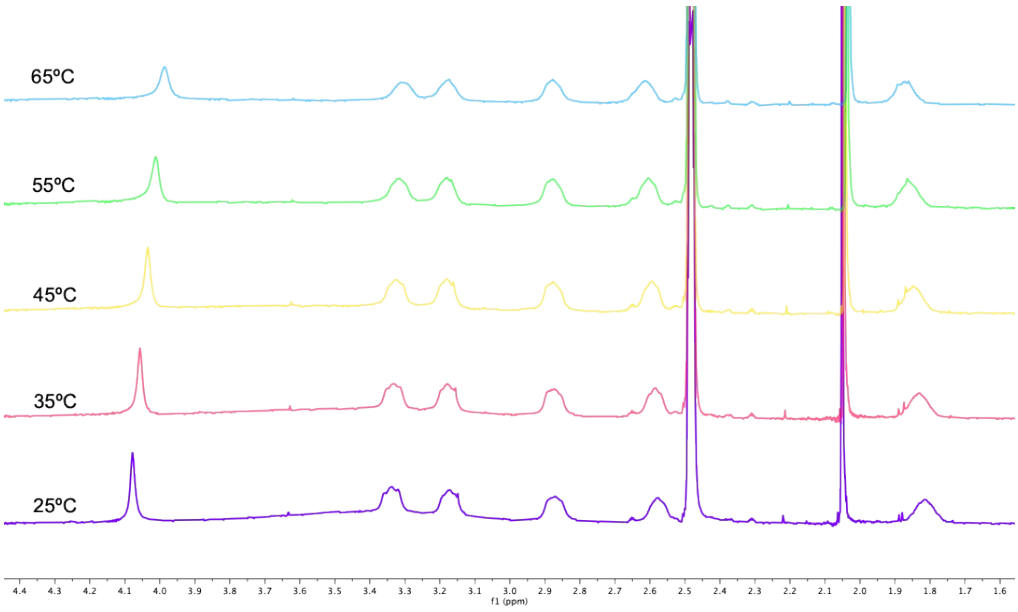

Figure S2. ^{1}H NMR spectra of **Cu$^{(I)}$(H$_2$NSNS2A)** in DMSO-d$_6$ acquired at different temperatures.

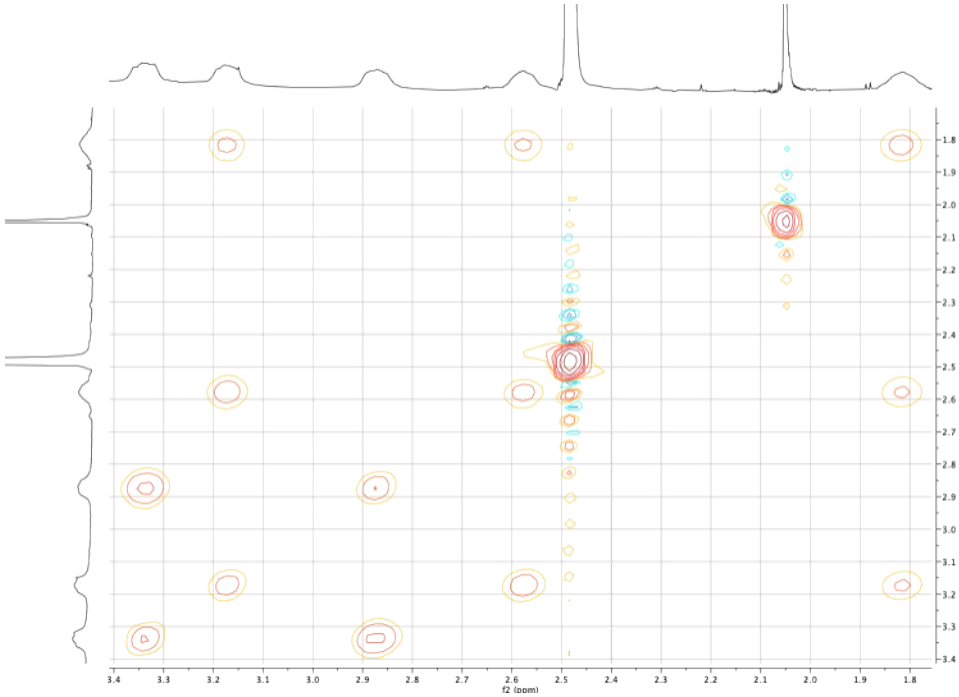

Figure S3. ^{1}H-^{1}H COSY NMR spectrum of **Cu$^{(I)}$(H$_2$NSNS2A)** in DMSO-d6 at 25°C.

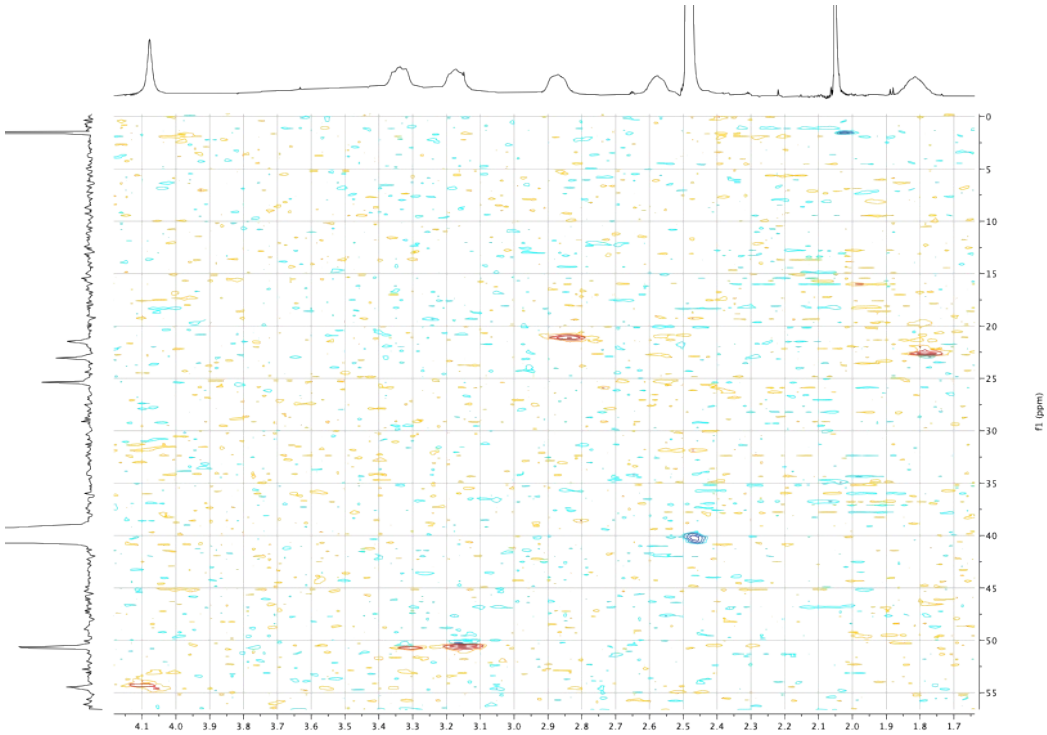

Figure S4. ^{1}H-^{13}C HSQC NMR spectrum of **Cu$^{(I)}$(H$_2$NSNS2A)** in DMSO-d6 at 25°C.

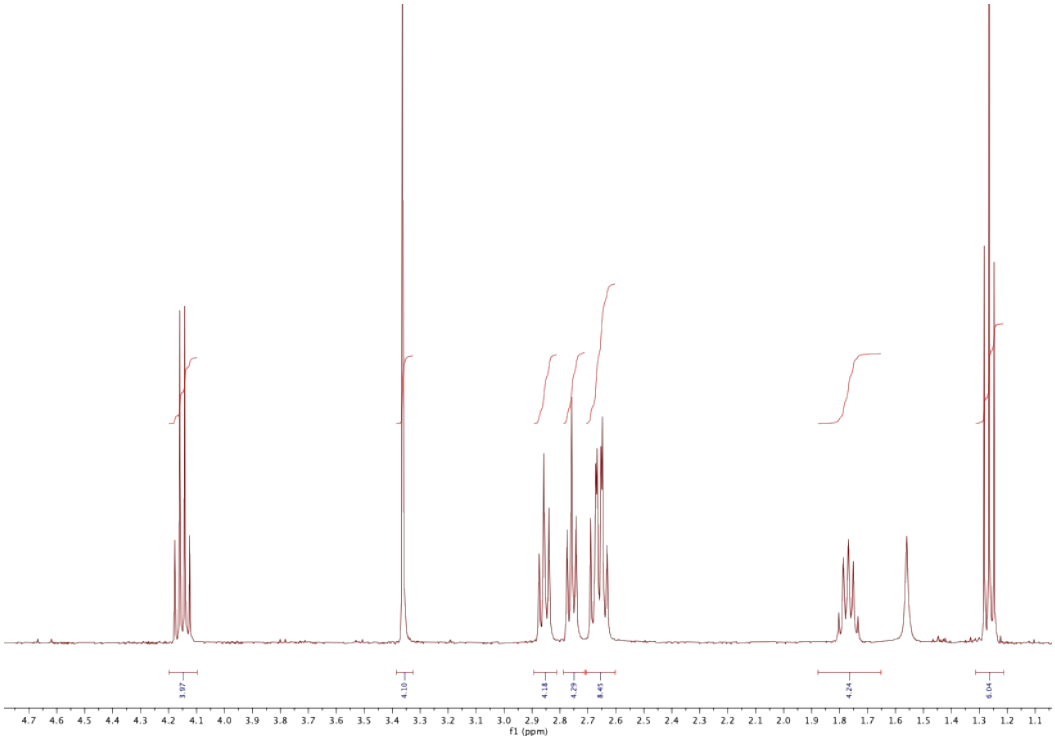

Figure S5. ^{1}H NMR spectrum of **1** in $CDCl_3$ at 25°C.

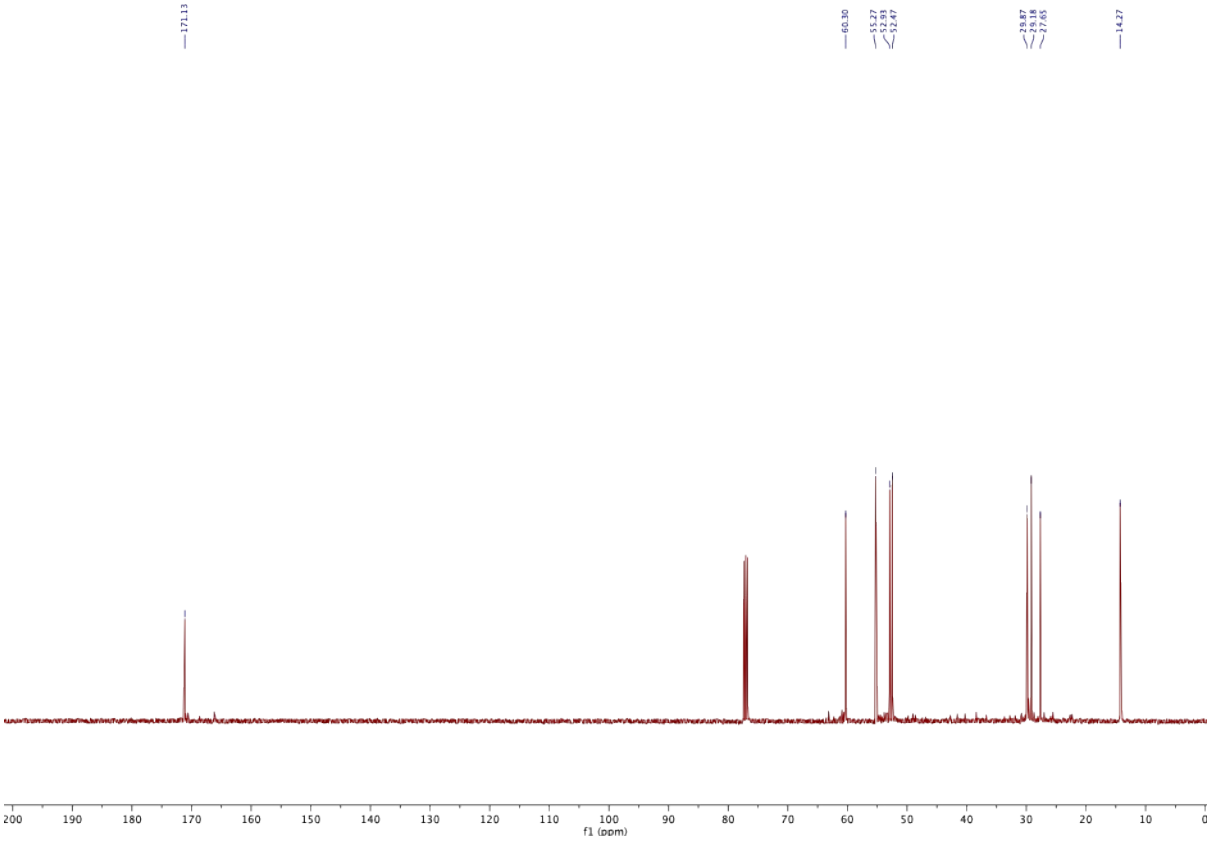

Figure S6. ^{13}C NMR spectrum of **1** in $CDCl_3$ at 25°C.

Figure S7. ^{1}H-^{1}H COSY NMR spectrum of **1** in $CDCl_3$ at 25°C.

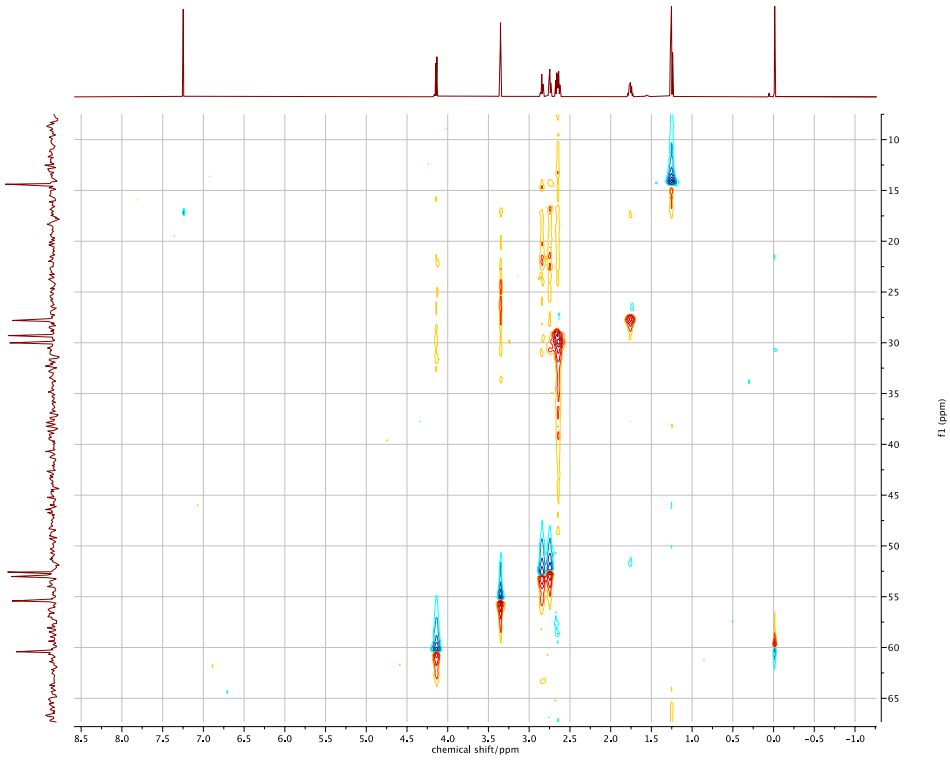

Figure S8. ^{1}H-^{13}C HSQC NMR spectrum of **1** in $CDCl_3$ at 25°C.

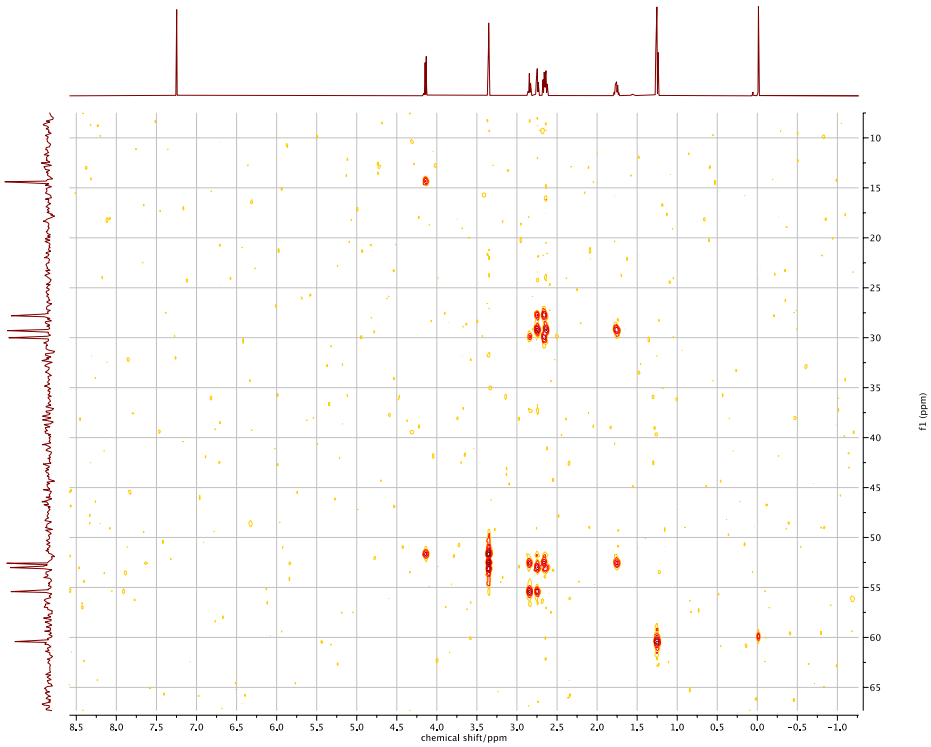

Figure S9. ^{1}H-^{13}C HMBC NMR spectrum of **1** in $CDCl_3$ at 25°C.

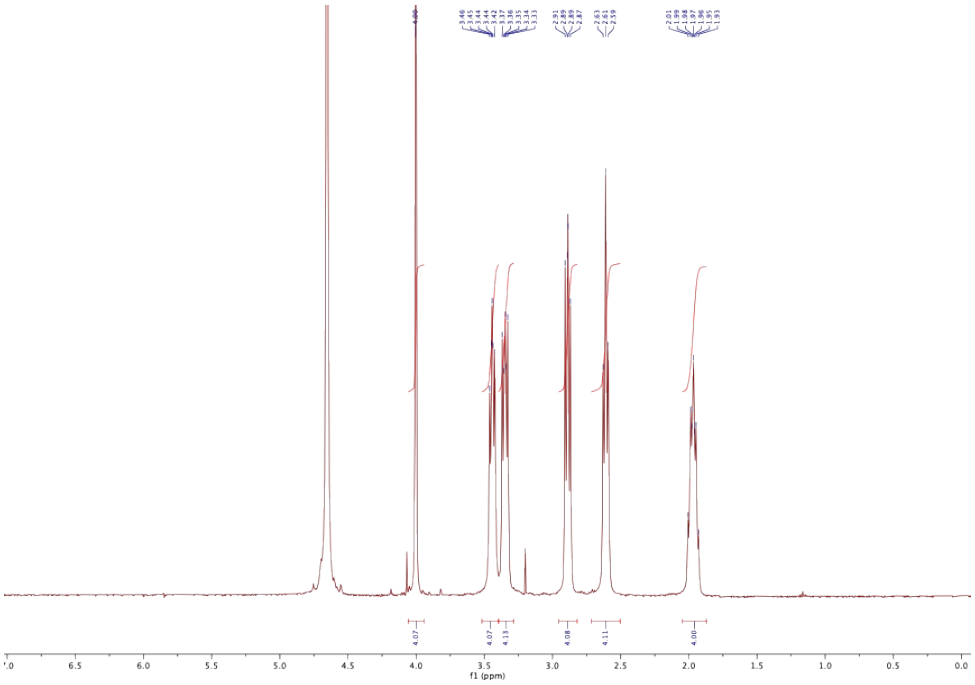

Figure S10. ^{1}H NMR spectrum of **2** in D_2O at 25°C.

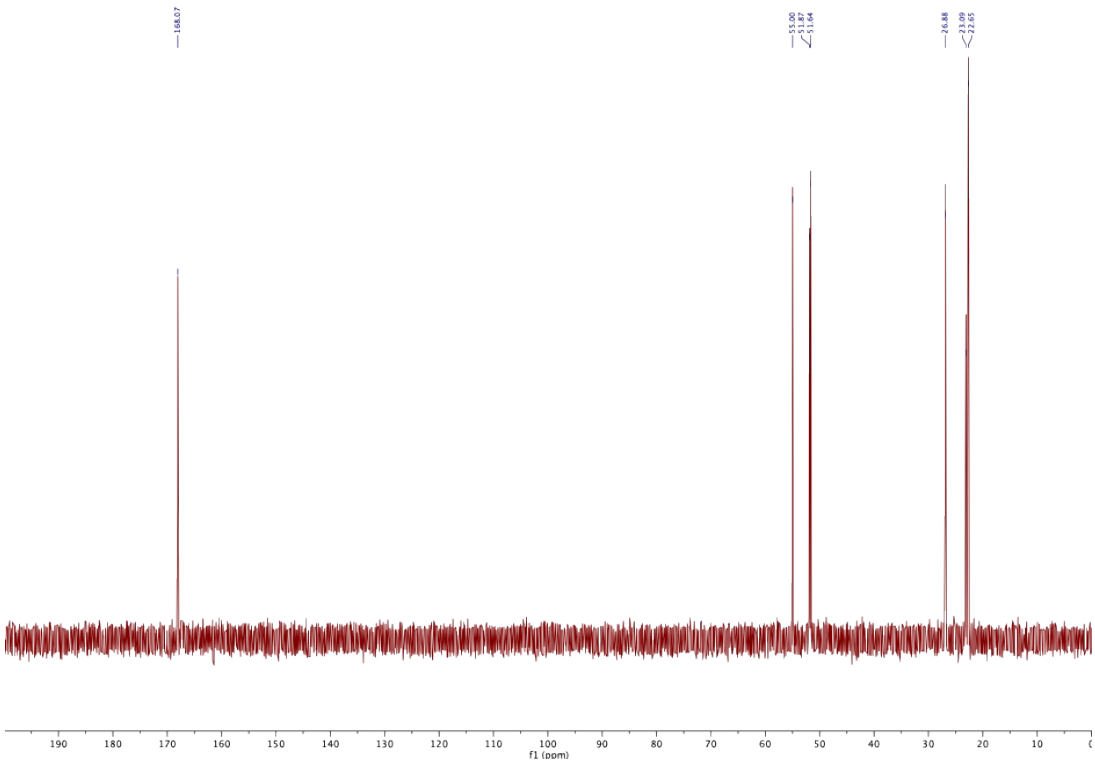

Figure S11. ^{13}C NMR spectrum of **2** in D_2O at 25°C.

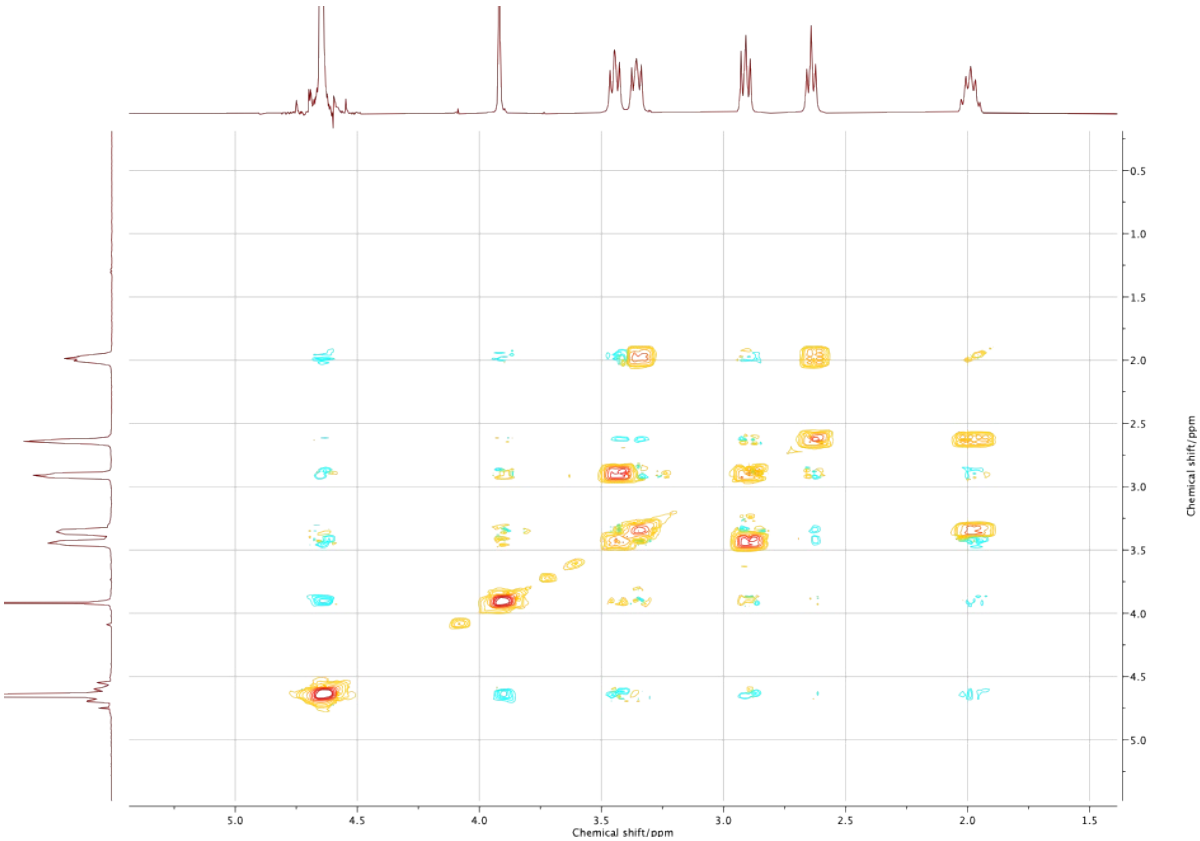

Figure S12. ^{1}H-^{1}H COSY NMR spectrum of **2** in D_2O at 25°C.

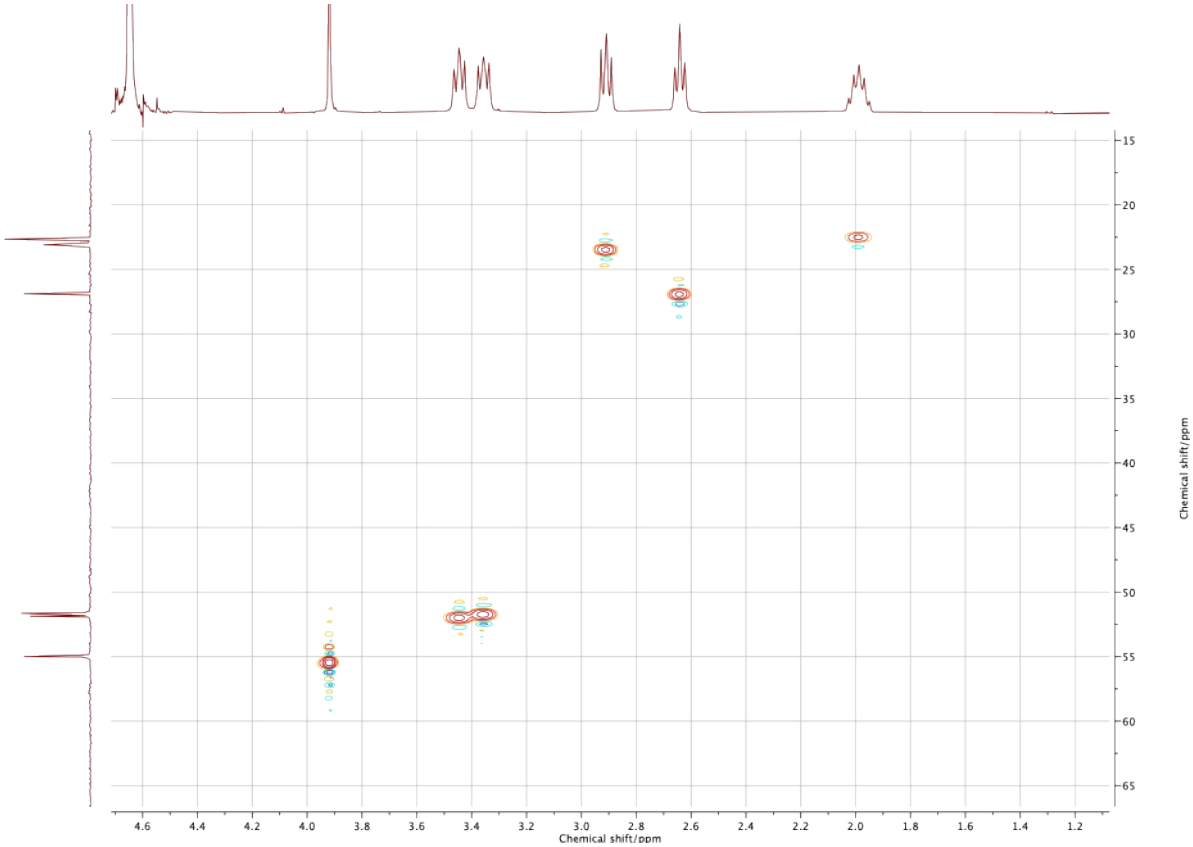

Figure S13. ^{1}H-^{13}C HSQC NMR spectrum of **2** in D_2O at 25°C.

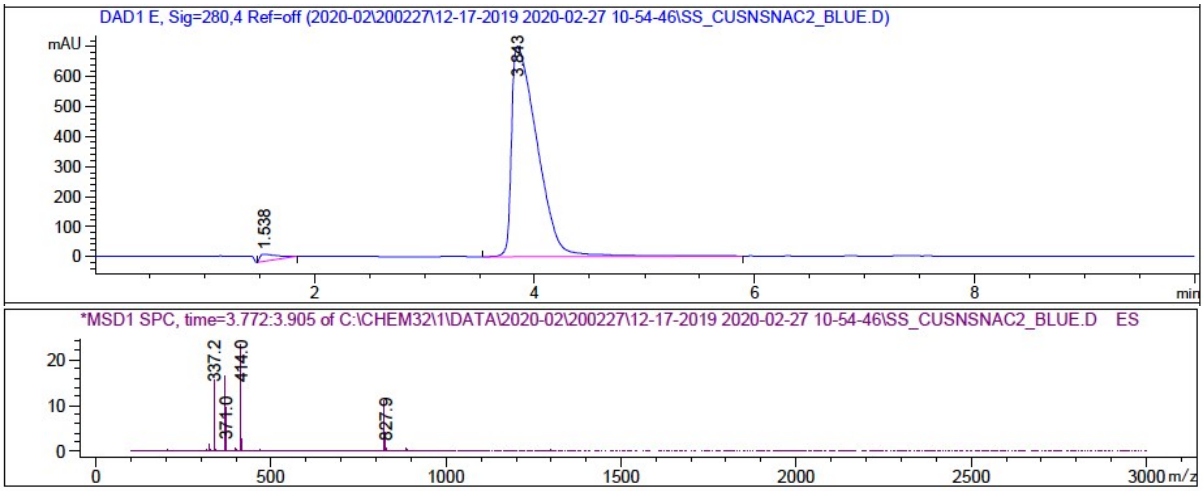

Figure S14. HPLC trace (top) of **Cu$^{(II)}$(NSNS2A)** and the corresponding ESI-MS signal (positive ion mode, bottom). Restek Ultra AQ C18 5 µm, 100 x 4.6 mm column. Solvent A - 50 mM ammonium acetate in water, solvent B – 90% acetonitrile/10% solvent A. 5%-95% solvent B over 6 min. Flow rate is 1 mL/min.

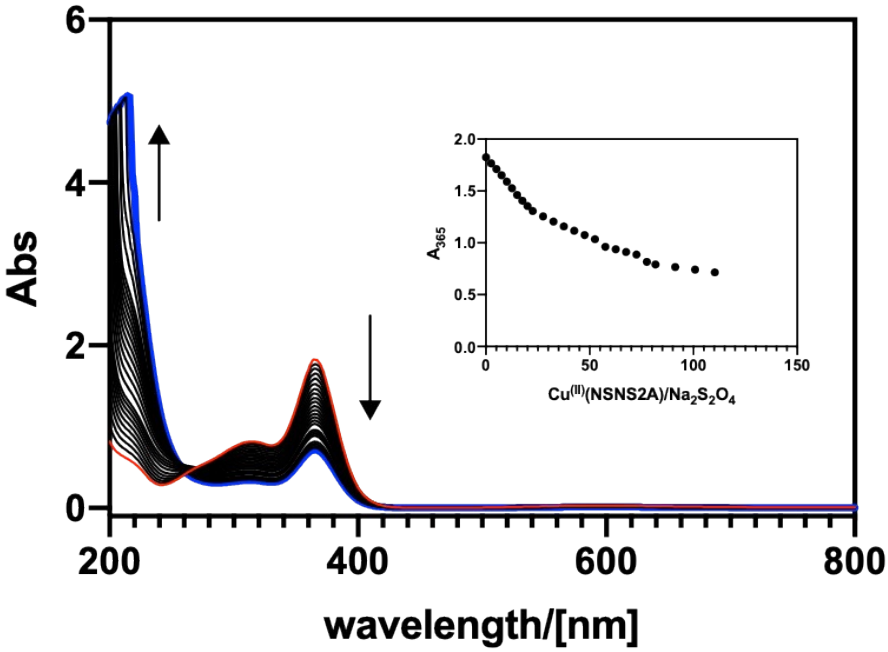

Figure S15. Change in the absorption spectrum of **$Cu^{(II)}$(NSNS2A)** upon addition of sodium dithionate (pH = 6.0).

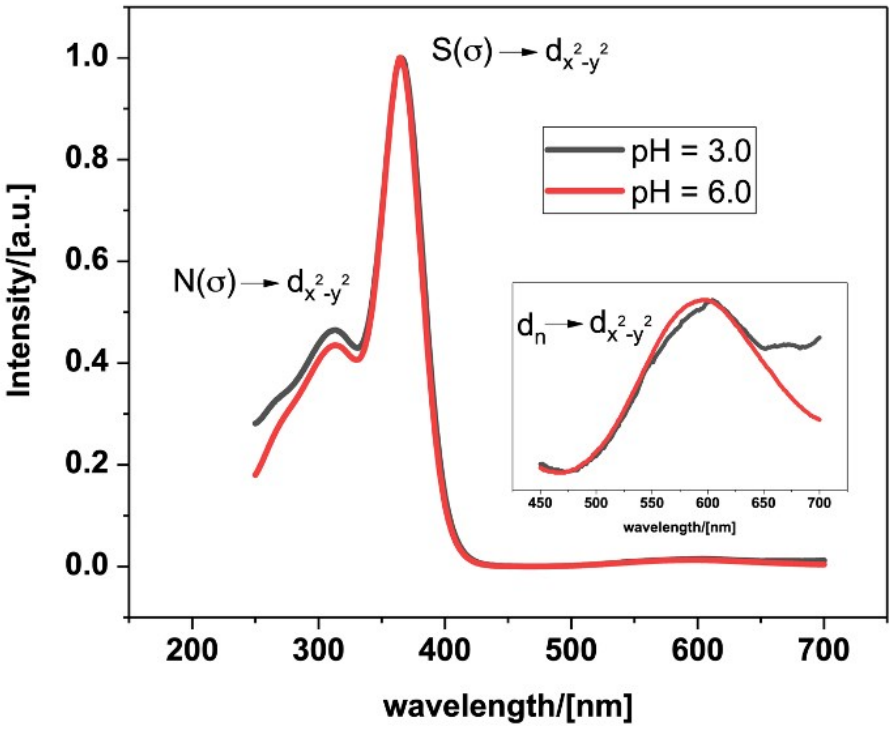

Figure S16. Absorption spectra of **$Cu^{(II)}$(NSNS2A)** at pH=3.0 (black) and pH=6.0 (red).

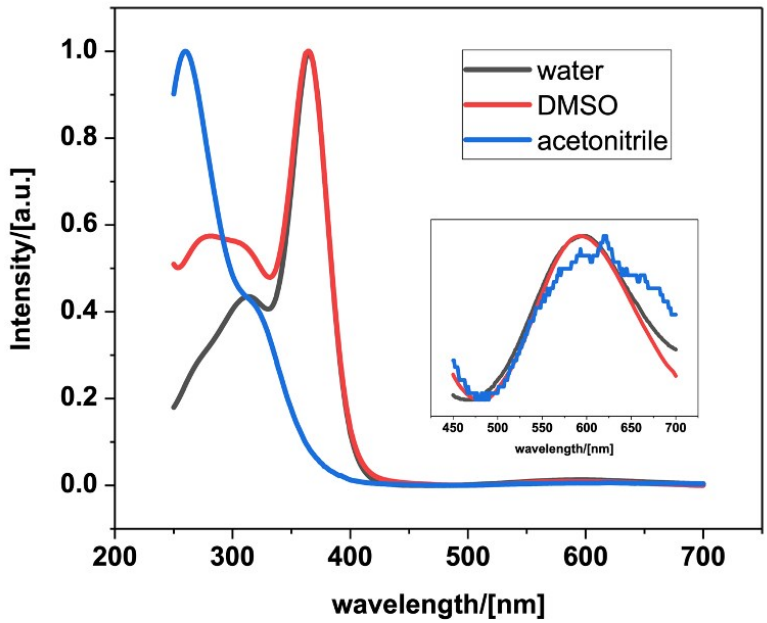

Figure S17. Absorption spectra of **Cu$^{(II)}$(NSNS2A)** in water (black), DMSO (red) and acetonitrile (blue).

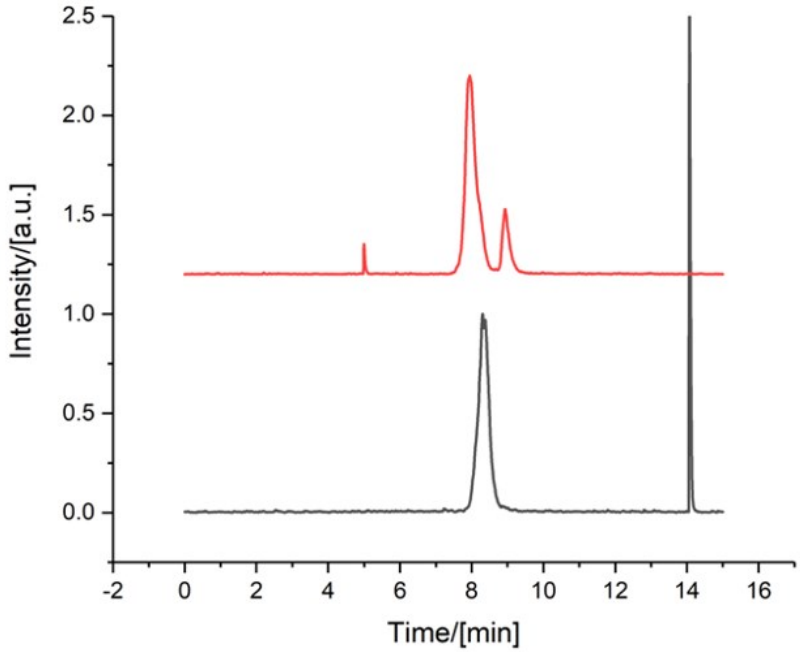

Figure S18. Radio-HPLC traces of **^{64}Cu$^{(II)}$(NSNS2A)** (bottom) and the mixture of **^{64}Cu$^{(II)}$(NSNS2A)** with **^{nat}Cu(ClO$_4$)$_2$** added (top). XBridge Amide 3.5 µm, 4.6 x 150 mm, solvent A – ammonium citrate solution in H_2O (20 mM, pH = 6.0), solvent B – 80% acetonitrile/20% solvent A. 100% solvent A over 0.5 min, then 0%-50% solvent B over 4 min. Flow rate is 1 mL/min.

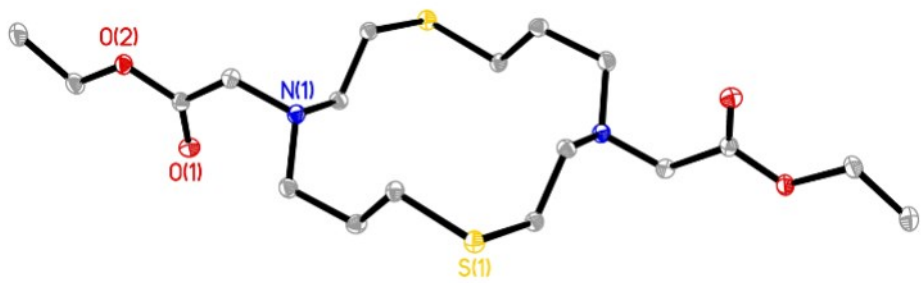

Figure S19. The thermal ellipsoid diagram showing the structure of the cationic unit for **1**. Hydrogen atoms are omitted for clarity. Thermal ellipsoids are set at 35% probability.

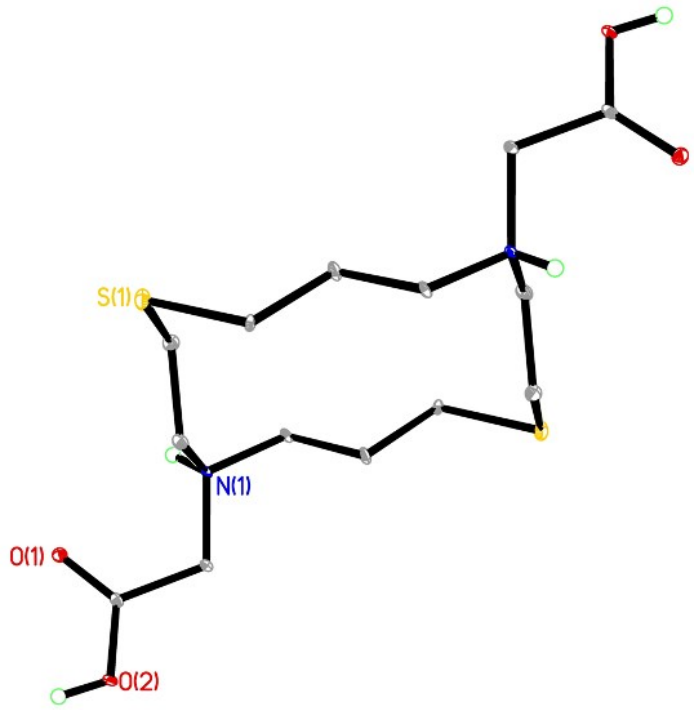

Figure S20. The thermal ellipsoid diagram showing the structure of the cationic unit $[H_2\mathbf{2}]^{2+}$ for a solid-state structure of 2•2HCl. Hydrogen atoms are omitted for clarity. Thermal ellipsoids are set at 35% probability.

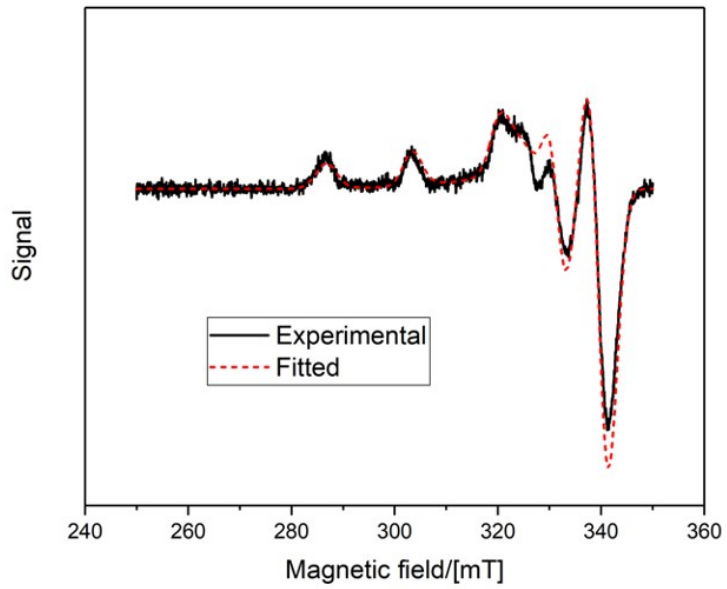

Figure S21. CW X-band EPR spectra (solid line) and fitted curves (dashed lines) for **Cu$^{(II)}$(NSNS2A)**. 45% glycerol/55% 0.1 HEPES solution (pH = 4.5), T = 77K.

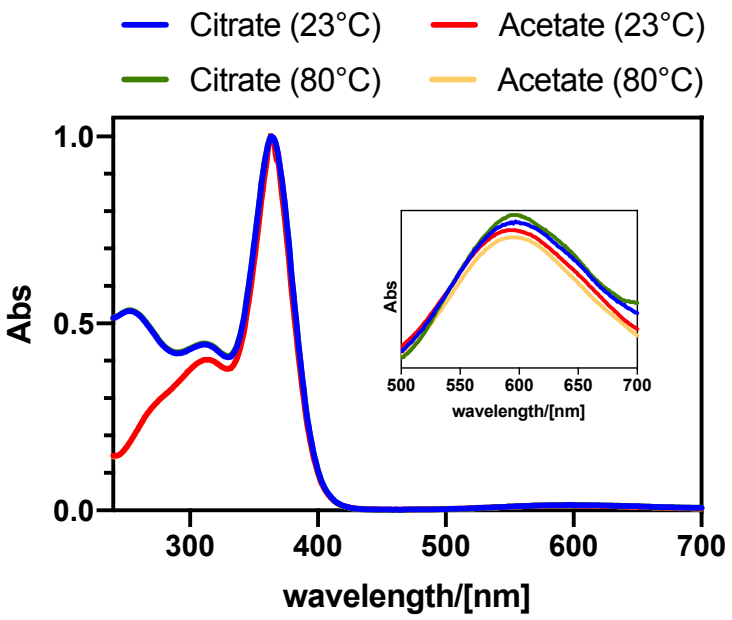

Figure S22. UV-vis absorption spectra of **Cu$^{(II)}$(NSNS2A)** prepared in acetate or citrate buffer. The inset shows the magnified region of the spectra corresponding to d-d transitions. The spectra were acquired in sodium acetate (40 mM, pH = 5.5) or ammonium citrate (0.3 M, pH = 6.0) buffers.

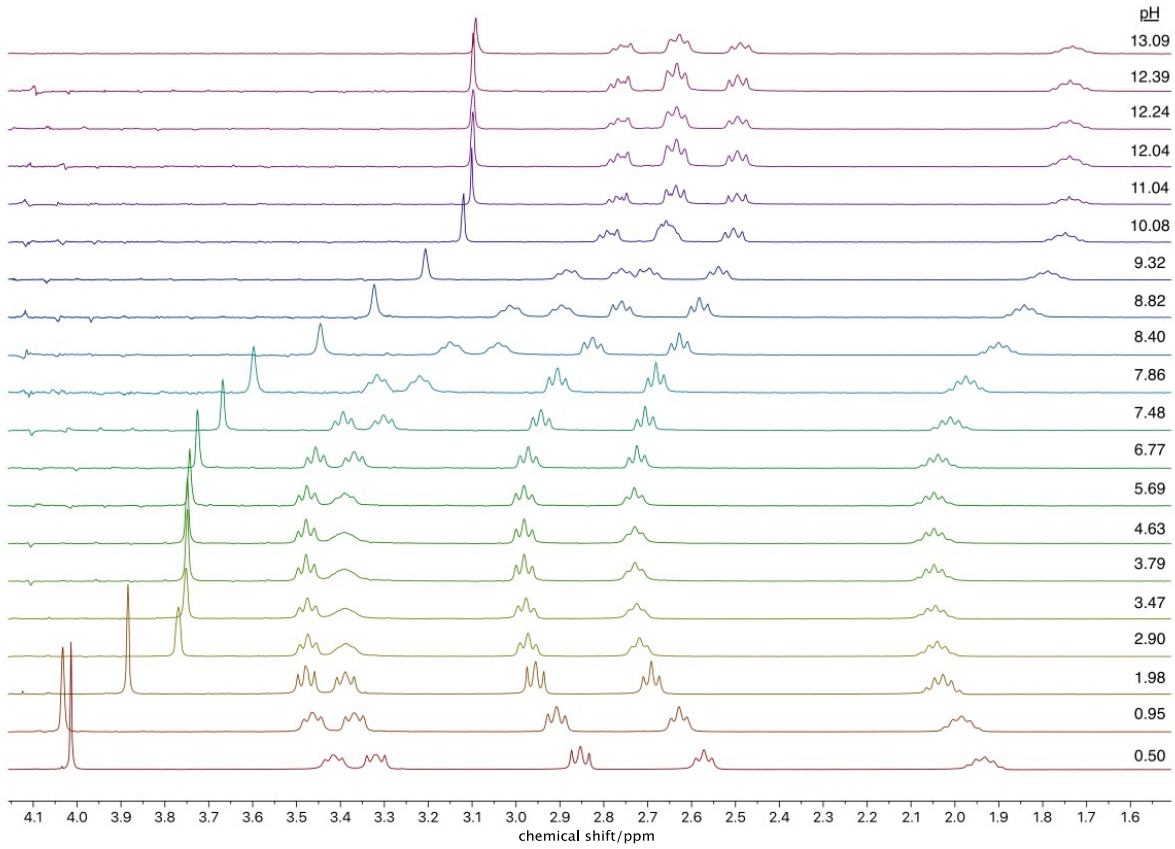

Figure S23. ^{1}H NMR spectra of **H_2NSNS2A** in D_2O at different pH values.

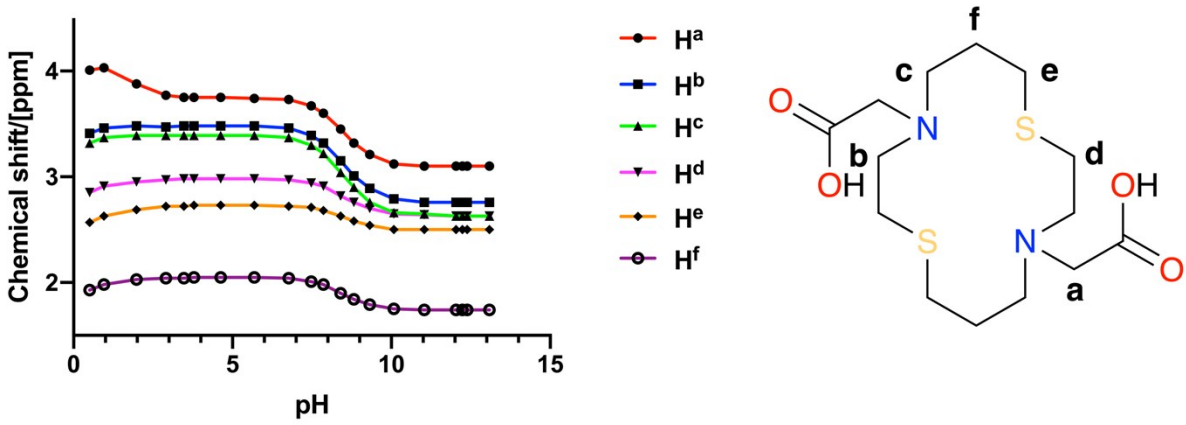

Figure S24. Variation of chemical shift values in **H_2NSNS2A** as a function of pH.

Table S1: X-ray crystal data and structure parameters for compounds **1-2** and **[Cu(1)](ClO$_4$)$_2$**.

Compound	**1**	**[H$_2$2]$^{2+}$**	**[Cu(1)](ClO$_4$)$_2$**
Empirical formula	$C_{18}H_{34}N_2O_4S_2$	$C_{14}H_{32}Cl_2N_2O_6S_2$	$C_{18}H_{34}Cl_2CuN_2O_{12}S_2$
CCDC	2003358	2003359	2003361
Formula weight	406.59	459.43	669.03
Crystal system	Triclinic	Triclinic	Monoclinic
Space group	P-1	P-1	P2$_1$/n
a/ Å	5.1763(4)	8.2747(5)	9.4305(4)
b/ Å	8.0757(6)	8.4428(5)	16.2613(8)
c/ Å	12.7460(10)	8.5526(5)	9.6556(5)
α(°)	92.297(5)	64.705(3)	90
β(°)	98.372(5)	89.681(3)	114.665(2)
γ(°)	96.965(5)	71.834(3)	90
Volume (Å^3)	522.34(7)	507.59(5)	1345.61(11)
Z	1	1	2
Dc (Mg/m^3)	1.293	1.503	1.651
μ (mm^{-1})	0.280	0.559	1.227
F(000)	220	244	694
reflns collected	9470	9216	12390
indep. reflns	2531	2508	3398
GOF on F^2	1.083	1.126	1.021
R1 (on F$_o^2$, I > 2σ(I))	0.0490	0.0667	0.0447
wR2 (on F$_o^2$, I > 2σ(I))	0.1202	0.2021	0.0974
R1 (all data)	0.0781	0.0734	0.0602
wR2 (all data)	0.1338	0.2080	0.1043

Table S2. Main UV-Vis spectra bands computed by TD-DFT (B3LYP/def2-TZVP) for optimised structure of **Cu$^{(II)}$(H$_2$NSNS2A)**, hydrogens are omitted for clarity.

Excited state	Energy (cm^{-1})	Wavelength (nm)	f_{osc}	Difference electron density between excited and ground state (blue –

				negative, red -positive) isovalue 0.01
5	23696	422	0.1589	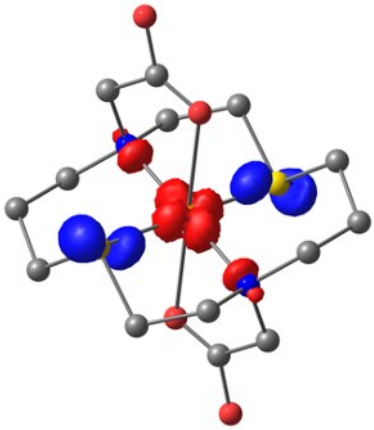
6	29297	341	0.1161	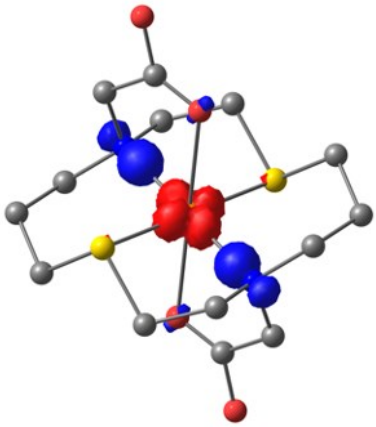
8	32215	310	0.0261	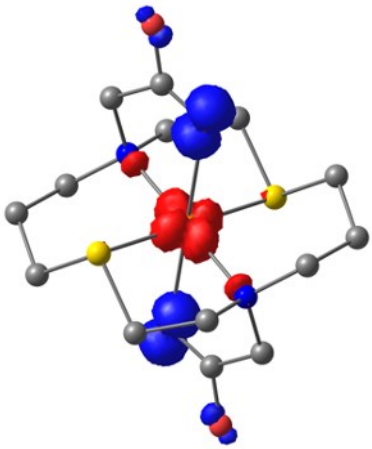
10	35827	279	0.0131	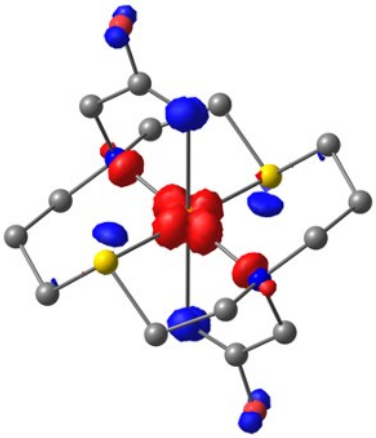

Table S3. Main UV-Vis spectra bands computed by TD-DFT (B3LYP/def2-TZVP) for optimised structure of **Cu$^{(II)}$(NSNS2A)**, hydrogens are omitted for clarity.

Excited state	Energy (cm^{-1})	Wavelength (nm)	f_{osc}	Difference electron density between excited and ground state (blue – negative, red -positive) isovalue 0.01
5	22828	438	0.0474	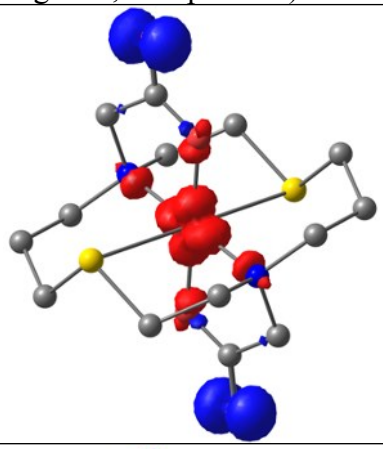
6	23606	424	0.0019	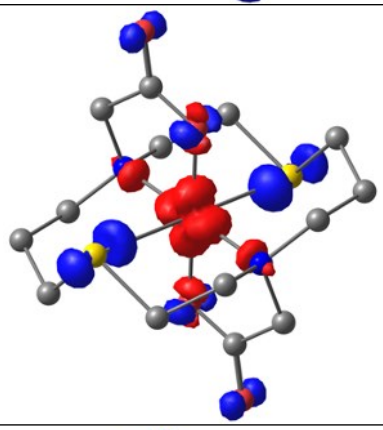
8	28599	350	0.0161	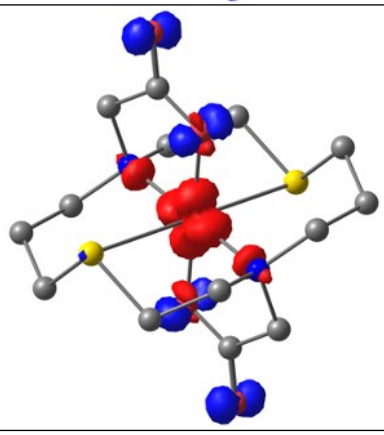

10	29077	344	0.0474	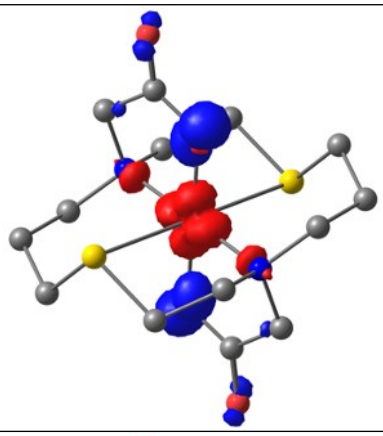
12	35241	283	0.1220